IET Radar, Sonar & Navigation

Research Article

IET Journals
The Institution of Engineering and Technology

Sky-wave over-the-horizon radar simulation tool

ISSN 1751-8784
Received on 7th April 2020
Revised 18th June 2020
Accepted on 21st July 2020
E-First on 15th September 2020
doi: 10.1049/iet-rsn.2020.0158
www.ietdl.org

Zenon Saavedra[1,2] ✉, Diego Zimmerman[1], Miguel A. Cabrera[1], Ana G. Elias[2,3]

[1]*Laboratorio de Telecomunicaciones, Departamento de Electricidad, Electrónica y Computación, Facultad de Ciencias Exactas y Tecnología, Universidad de Tucumán (FACET-UNT), Av. Independencia 1800, 4000 Tucumán, Argentina*

[2]*Consejo Nacional de Investigaciones Cientificas y Técnicas, CONICET, Argentina*

[3]*Laboratorio de Física de la Atmósfera, Dpto. de Física, FACET, UNT, INFINOA (CONICET-UNT), Av. Independencia 1800, 4000 Tucumán, Argentina*

✉ *E-mail: zsaavedra@herrera.unt.edu.ar*

Abstract: This work deals with the entire process of target detection and ranging by a sky-wave over-the-horizon radar (OTHR) computational model simulation. The different processing stages of the transmitted signal along its space–time trajectory from transmission to digital signal processing are modelled. With this simulation tool a moving target present over the sea can be detected according to a set of given initial conditions together with the ionosphere model inputs and the target electromagnetic model. Initial conditions as well as the modulation and filtering options among other parameters of the model can be set easily. The present work is intended to be a further contribution to OTHR studies, providing a user-friendly tool of easy application in order to improve a radar design, facilitate its implementation, as well as for debugging algorithms and signal processing techniques.

1 Introduction

A sky-wave over-the-horizon radar (OTHR) works through reflections in the Earth's ionosphere to detect targets beyond the horizon. Therefore, it largely depends on the state of the ionosphere [1, 2]. The performance of these radars also depends on other factors such as the transmitter and receiver characteristics, the radar cross-section (RCS), clutter, external noise, the waveform choice and the signal processing techniques, all of which can be modelled depending on application requirements [3–5].

Saavedra *et al.* [6] developed a model for the first radar processing stage of target detection. From this model, the parameters needed for the digital signal processing (DSP) of the received signal are obtained. As a continuation of the work by Saavedra *et al.* [6], these parameters are used to generate the received signal time series. Through iterations of this process, multiple received signals are obtained and converted to a matrix. After the pulse compression, a DSP technique is applied, with several options for settings, in order to finally detect the target's position within a sea searching scenario.

A GNU-Radio, which is an open-source Software Defined Radio platform for radar applications and Python language, is used in the processing stages from the reception to DPS.

The synthesis of the received signal and each step from its transmission modelling are described in Section 2, followed by the pulse compression technique in Sections 3 and the DSP in Section 4. A simulation example and concluding remarks are presented in Sections 5 and 6.

2 Received signal: from transmission to digital synthesis

For performing the target detections within a searching area on the sea surface, the echo signals received by the radar are synthesised through the models described below.

2.1 Propagation model

Consider a radar transmitted signal, which propagates through the ionosphere of Earth, which is reflected, and reaches a target that retransmits part of the energy to the radar. Fig. 1 shows an outline of this process described in [6]. From this model, the parameters to generate the received signal time series are obtained [7]. The parameters are round trip delay, clutter power, noise power, echo power, Bragg frequency total attenuation etc.

The transmitted signal, $S_T(t)$, is given by (1):

$$S_T(t) = u(t)A(t)m(t)e^{j\omega t + \varphi} \tag{1}$$

where $u(t)$ is a rectangular pulse and defines the transmission and reception times, $A(t)$ is the transmitter power–gain ratio, $m(t)$ contains the modulation type, and ω and φ are the initial frequency and phase of the transmitted signal, respectively.

The transmitted signal illuminates a certain area on the sea surface and a portion of the energy is reflected towards the radar, that is the received signal, $S_R(t)$ [8], given by (2):

$$S_R(t) = a_t(t)\mathrm{RCS}(t)A_R(t)u(t-\tau_R)A(t)m(t)e^{j\omega t+\varphi}e^{\pm j\omega_d t+\theta}e^{\pm j\omega_B t} \tag{2}$$

where $a_t(t)$ is the attenuation on the way back and forth, $A_R(t)$ is the receiver directive gain [as well as $A(t)$ is a function of elevation angle, which in turn will vary with both range and ionospheric virtual height], $\mathrm{RCS}(t)$ is the radar cross-section of the target, ω_d is the target's Doppler frequency, τ_R is the round trip delay, θ is the phase shift due to propagation through the ionosphere and ω_B is the Bragg frequency associated with the sea, and the exponential describes a complex sine or cosine function.

On the other hand, adding to the average value one kind of probability density function (PDF), the random character of generated signal is incorporated. For example, the RCS has a Swerling I, II, III or IV PDF, the noise has a lognormal and the PDF of clutter can be Rayleigh.

The transmitting and receiving antennas are considered as ideal directional antennas (with a determinate gain, polarisation and main, side lobes), and also a monostatic radar system.

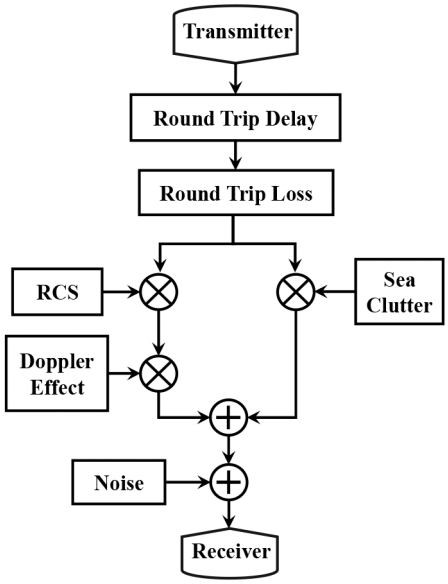

Fig. 1 *Propagation model block diagram*

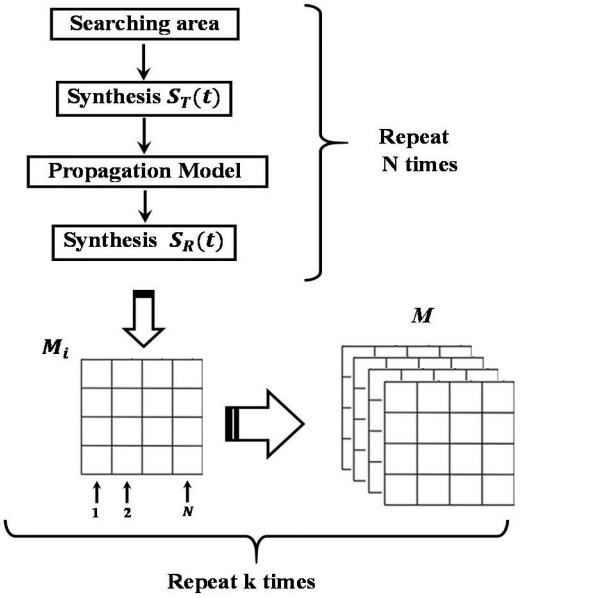

Fig. 2 *Transmission and reception block diagram model together with its output matrix* ***M*** *composed of N × k received signals. k: number of cells within a DIR; N: number of transmitted signals per cell*

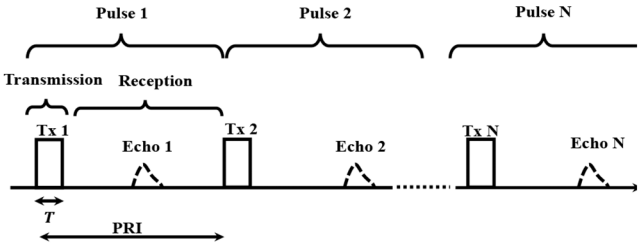

Fig. 3 *Scheme of N pulses transmission of time length T and PRI*

2.2 Transmission and reception process model

The searching area is divided into dwell illumination regions (DIR), which in turn are divided into k resolution cells. The transmission and reception process is repeated N times per cell. These N signals are received within a coherent integration time and then arranged within a two-dimensional (range and pulse) matrix $\boldsymbol{M_i}$. At the end of a DIR, search k matrices are obtained as follows: $\boldsymbol{M}_1, \boldsymbol{M}_2, \ldots, \boldsymbol{M_k}$, which make up matrix $\boldsymbol{M}$ of dimension $N \times k$.

Fig. 2 shows the complete transmission and reception process model, from which $\boldsymbol{M}$ is obtained.

Fig. 3 shows the N pulses, which are transmitted per cell, with a pulse time length, T, and a pulse repetition interval (PRI).

3 Pulse compression

A key factor in the radar performance is pulse compression, which generally uses frequency or phase modulations [8]. In our tool, both modulations, linear frequency modulation in the first case and binary phase-shift keying (BPSK) and quadrature phase-shift keying in the second case, are applied.

3.1 Linear frequency modulation

This modulation, also called chirp, consists of a certain duration T during which the carrier frequency increases or decreases linearly so that $m(t) = \exp[\mathrm{i}\Phi(t)]$ [9] and $\Phi(t)$ is given by (3):

$$\Phi(t) = 2\pi\left(f_c t + bt^2\right), \quad -\frac{T}{2} \le t \le \frac{T}{2} \tag{3}$$

where f_c is the carrier frequency at $t = 0$, b is the chirp rate and is calculated as $\left(b = B/T_{\text{chirp}}\right)$, T_{chirp} is the duration of chirp and B is the bandwidth.

3.2 Phase modulation

Phase modulation can be bi-phase, with two possible states, or poly-phase, with more than two. The radar's detection performance depends, among other variables, on the phase code design [9]. Regarding duration, a better resolution is obtained with a shorter pulse. Also regarding correlation, in many cases, a criterion for a code selection is to use codes that have an autocorrelation function with a well-defined main lobe and minimum lateral lobes. For example, Sulzer and Woodman [10] showed that the energy in the lateral lobes of the correlations must be 20% or less than that of the main lobe to achieve good detection quality. The phase codes that can be selected in the proposed model are listed in Table 1.

The use of transmitted signal coding techniques favours the signals that were encoded and can suppress those signals that were not.

3.2.1 Bi-phase codes: Bi-phase codes have a phase that changes between only two states. They are characterised by having a low tolerance to Doppler, which implies that for high Doppler values, the code loses its autocorrelation property. The bi-phase code options in our model are Barker [8] and Golay or auto-complementary codes [10, 11], both are described in Table 1.

3.2.2 Poly-phase codes: Poly-phase codes have more than two possible phases, thus achieving a better tolerance to Doppler, compared to bi-phase codes. Among the several options of poly-phase codes commonly used, the Frank codes are used in our model [12]. The three Frank options are described in Table 1.

4 Digital signal processing

The first step before applying digital processing is to receive the signal $S_{\text{R}}(t)$ with a receptor implemented in a Radio Defined Software. The receptor has a mixer, two gain blocks of 50 and 30 dB and filters to attenuate the unwanted signal. After that, the set of signals received are stored in the matrix $\boldsymbol{M}$. These signals can be strongly attenuated presenting a highly degraded signal-to-noise ratio (SNR). To extract the useful information, DSP [13] techniques are applied to reduce noise, clutter and to cope with attenuation. Fig. 4 shows a block diagram of this process. Each block is described below.

Table 1 Phase code options for phase modulation

Code type	Code name	Code
bi-phase	auto Comple.	[1,1,0,1,1,1,1,0,1,0,0,0,1,0,1,1]
		[1,1,0,1,1,1,1,1,0,0,1,1,1,0,1,0,0]
bi-phase	Barker 7	[1,1,1,0,0,1,0]
bi-phase	Barker 11	[1,1,1,0,0,0,1,0,0,1,0]
bi-phase	Barker 13	[1,1,1,1,1,0,0,1,1,0,1,0,1]
poly-phase	Frank 1	[1,1,1,-1]
poly-phase	Frank 2	[1, 1, 1, 1, − 0.5 + 0.87j, − 0.5–0.87j, 1, − 0.5–0.87j, − 0.5 + 0.87j]
poly-phase	Frank 3	[1,1,1,1,1,1j,−1,−1j,1,−1,1,−1,1,−1j,−1,1j]

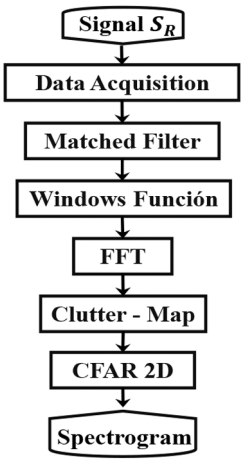

Fig. 4 *DSP block diagram*

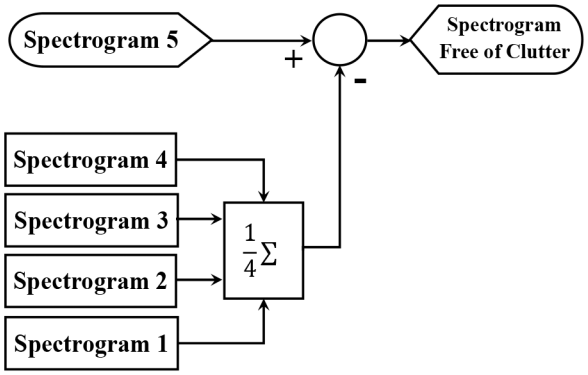

Fig. 5 *Flowchart of clutter-map processing*

4.1 Matched filter

Adaptive filtering allows finding patterns in a degraded or noise received signal, with a self-adjusting transfer function and identifying the transmitted pulse.

The transfer function used in our case is a conjugated time-reversed version of the transmitted signal, which maximises the SNR [8]. The filtered signals are arranged again in the matrix $\boldsymbol{M}$.

4.2 Window function

A time-domain window function is applied to reduce edge effects which result in spectral leakage in the fast Fourier transform (FFT). Side lobes in the frequency spectrum are attenuated in this way. In our model, the Kaiser (or Kaiser–Bessel) window function, which is a good option for general purpose, whose shape can be changed by its only parameter β, and this window is applied to each row of the matrix $\boldsymbol{M_i}$.

For example, for $\beta = 1$ the main lobe is spread up to around 0.05 Hz, and in 20 dB are attenuated the side lobes. On the other hand, with $\beta = 9$ the main lobe is spread up to around 1.1 Hz, and in at least 70 dB are attenuated the side lobes. Now, in an OTHR system that operates with Doppler frequencies in the range of 0−2 Hz, a value equal to 31 is taken by the adjustable parameter β of the Kaiser window.

4.3 Fast Fourier transform

FFT is applied to each row of the $\boldsymbol{M_i}$ matrices, in order to consider the existing transitions between the N pulses corresponding to the same resolution cell. Finally, after applying the FFT, we proceed to sum all the rows in $\boldsymbol{M_i}$, and in that way the total frequency spectrum of the analysed resolution cell is obtained.

4.4 Clutter map

The target under search is immersed in an environment that has a significant clutter component. To perform the filtering in order to obtain a reliable detection of the moving target, an average frequency spectrum is estimated using successive DIR scans, which constitutes the clutter map [8, 14, 15]. Since the searching area is over the sea the clutter is associated with the Bragg Doppler component, which has a relatively constant peak in the spectrum due to its slow variations, so that the averaging technique seems to be a good choice.

On the other hand, it is worthwhile noticing that the Bragg peak amplitude may have a low variance but its Doppler, controlled by ionospheric path, may move significantly. It can also be spread by multipath illumination. Also, as positive and negative Bragg lines are resolved, their amplitude will depend on the wind direction, which may not be constant over the observation area.

Regarding this last aspect, the wind direction contribution was evaluated as a constant attribute of the model over the entire observation area.

The clutter map is constructed averaging the spectrums, which result from four consecutive scans. The target velocity must be sufficiently high to allow the target to move into neighbour resolution cell between scan to scan of the cells to avoid being part of the clutter map.

The search is performed with the fifth scan from which the clutter map is subtracted to finally obtain a clutter-free map where the target can be a highlight. A block diagram of this process is shown in Fig. 5.

4.5 Constant false alarm rate (CFAR)

In order to achieve the robust behaviour and performance, an adaptive threshold called cell averaging CFAR in the 2D is used for the detection. This method permits an automatic determination of an adaptive threshold. After that, if the test sample is greater than the threshold, this sample is considered to be a real target.

The aim of the method is to adjust the threshold value in order to ensure that the probability of the false alarm remains in the desired value [8].

5 Simulation and result

The implemented simulation tool has two interphases. The first interphase, shown in Fig. 6, serves to obtain the set of parameters needed for synthetically generate signals from a set of initial conditions defining the transmitter and the search scenario. The second interphase, shown in Fig. 7, uses the output of first interphase among other parameters which are needed for signal processing and target detection.

The fictitious scenario is described in Table 2. On the coast of the province of Chubut, Argentina the OTH radar is located, as shown in Fig. 8. The input parameters given in Tables 2 and 3 are used in the first interphase, which are given as output parameters in Table 4.

A DIR area is considered, with a minimum range of 1100 km and a maximum range of 1600 km. With a bandwidth of 10 kHz, a range width of resolution area of $\Delta R = 15$ km is obtained, which requires 33 resolution cells to sweep the area entirely.

With the parameters listed in Table 4 and after applying the transmission and reception process modelling, the matrix $\boldsymbol{M}$ is obtained, which contains all the signals received within the same DIR.

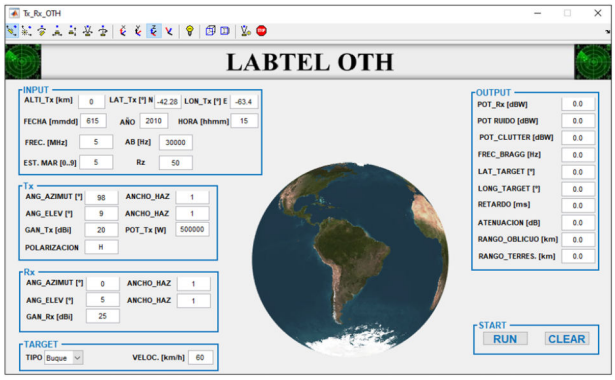

Fig. 6 *First user interphase. Transmitter and search scenario parameters are input in the left side windows. Output data appear in the right side window*

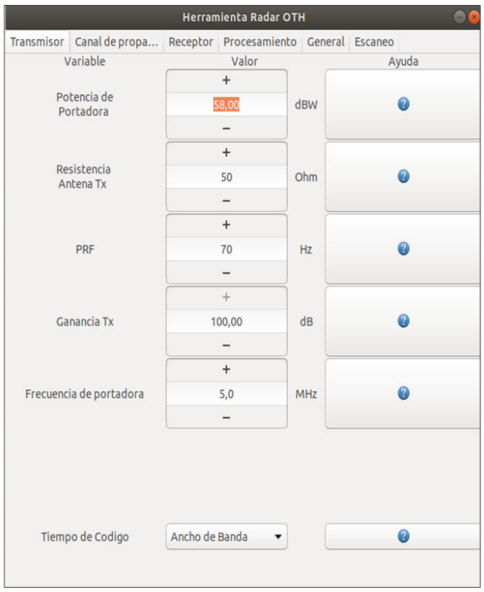

Fig. 7 *Second user interface that will generate the transmitted signal, synthesise the received signal, and process it, using input parameters obtained from the first interphase*

Table 2 General parameters that define the transmitter (OTHR) and searching scenario parameters

Parameter	Value
Pos. Geo. transmitter	Lat. 42.3 S Long. 63.4 E
date, time	15/06/2010, 15:00 pm
frequency	6 MHz
polarisation	horizontal
bandwidth	10 kHz
elevation angle	3–9°
elevation angle beamwidth	1°
azimuth angle	98°
azimuth angle beamwidth	3°
transmitted power	500 kW
antenna's gain Tx, Rx	20 dB, 25 dB
sea state	state: 3
see cross-section	$\sigma_0 = -29\,\text{dB/km}$

The following values were adopted in this example for Barker 11 code: modulation: BPSK; AB: 10 kHz; PRI: 1/40 Hz; length code: 13; number of integrations, N: 300; $P_{\text{Fa}} = 1 \times 10^{-10}$ and a Doppler frequency value for the target speed of 0.16 Hz ($v_{\text{D}} = 15\,\text{km/h}$, $f_{\text{c}} = 6\,\text{MHz}$). The next step is to apply DSP.

Fig. 9 presents the spectrograms before and after the clutter map, together with the final detection. After the detection, to transform the slant coordinates to ground coordinates, a coordinate registration geometric method is applied.

Fig. 8 *OTHR geographic location in South America, together with the search scenario*

Table 3 Input parameters on the first interphase, these belong to target

Parameter	Value
speed target	15 km/h
kind of target	fishing vessel
target orientation	azimuth: 10°
Geo. Pos. target	Lat. 42.58 S Long. 45.18 E (R = 1400 km from radar)

Table 4 Received signal parameters obtained from the first interphase

Parameter	Value
target power	−233 dBm
noise power	−118 dBm
clutter power	−211 dBm
bragg frequency	± 0.27 Hz
total attenuation	−369 dB
target delay (round trip)	9.95 ms

We obtained two detections. The detection between $R_{\text{min}} = 1395\,\text{km}$ and $R_{\text{max}} = 1410\,\text{km}$, which corresponds to resolution cell 20, is our target, and the other detection (cell 16) is a false alarm. It means that the clutter-map method is effective, allowing the correct mitigation of the clutter, which finally allows the target detection, but on the other hand, we need to improve the CFAR.

6 Conclusion

The simulation tool presented in this work adequately models all OTHR stages from signal transmission, propagation and reception to DSP in a fast and intuitive way. The proposed tool can be widely used for research and sky-wave OTHR development projects, as well as in system calibration.

While some simplifications were adopted, the system is an excellent starting point to study and analyse these kinds of systems. The number of variable parameters makes the software versatile, allowing the study of OTHR behaviour in a wide range of scenarios. In addition to the possibility of modifying the transmitter and search scenarios, it is also possible to configure the DSP.

Based on a large number of simulations for different target Doppler values (one of which is presented here as an example), we consider that the digital processing techniques are used adequately to fulfil the purpose of detecting sea moving targets.

Having used the GNU Radio Companion environment, the proposed work can be exported to a Software Defined Radio easily.

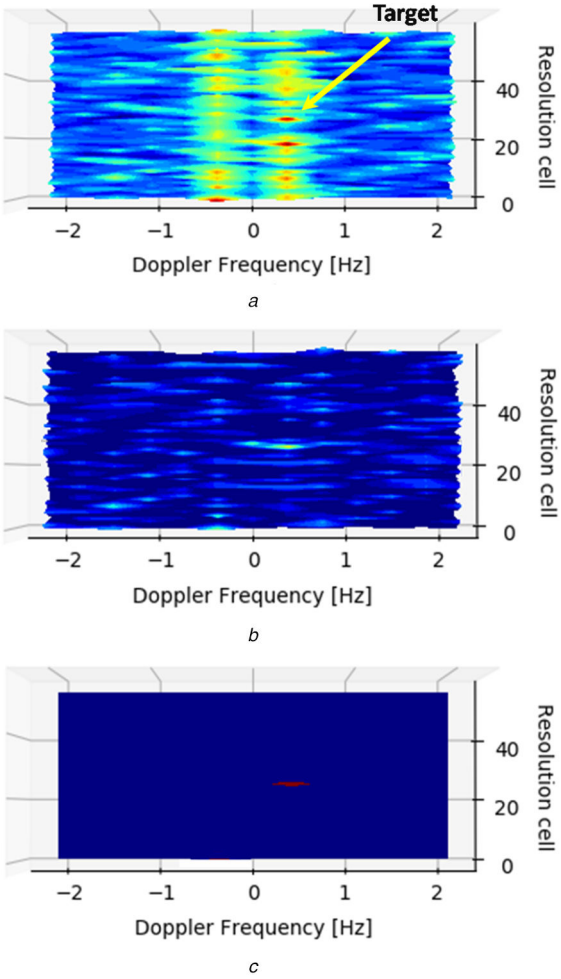

Fig. 9 *Simulation result for a target Doppler frequency = 0.16 Hz*
(a) Spectrum of the searching scan, ***(b)*** Spectrum obtained from (a) after subtracting clutter map which results from a previous four spectrum average, ***(c)*** Detection where the red area corresponds to the target

This is extremely useful and can be exploited, considering the high potential and great development that these kinds of devices are undergoing recently.

From the comparison between our tool and that present in Cervera *et al*. [3], we observed the following principal differences: we work with temporal series and Cervera by contrast only working with average values, and it does not use any probability distribution function. Both models use an electromagnetic software to determine the RCS of a target, but in our case the model uses all results of the simulation and Cervera, by contrast, uses only the average RCS simulation. Finally, Cervera does not implement any digital processing to the target detection and analyses the SNR only.

From the above, it is concluded that the proposed tool has a series of advantages, which makes its use worthwhile; on the other hand, our tool is nearer to realistic behaviour of an OTHR. Certainly, this tool can be improved by surpassing each phase as well as adding neglected aspects through additional options such as meteorological characteristics and therefore noises, as well as the option for importing real data (e.g. GPS coordinates of a target and its velocity), which are planned as future work.

7 Acknowledgments

We thank the CONICET (Argentina), by the Doctoral Scholarship of Zenon Saavedra, Universidad Nacional de Tucumán (Argentina) and Agencia Nacional de Promoción Científica y Tecnológica (Argentina) for the grants through the Projects PICT2015-0511 (Argentina).

8 References

[1] Skolnik, M.I.: '*Radar handbook*' (McGraw-Hill, USA, 2008, 3rd edn.)
[2] Zolesi, B., Cander, L.R.: '*Ionospheric prediction and forecasting*' (Springer-Verlag, Berlin, 2014)
[3] Cervera, M.A., Francis, D.B., Frazer, G.J.: 'Climatological model of over-the-horizon radar', *Radio Sci.*, 2018, **53**, pp. 988–1001
[4] Francis, D. B., Cervera, M. A., Frazer, G. J.: 'Performance prediction for design of a network of skywave over-the-horizon radars', *IEEE Aerosp. Electron. Syst.*, 2017, **32**, pp. 18–28
[5] Anderson, S.: 'OTH radar phenomenology: signal interpretation and target characterization at HF', *IEEE Aerosp. Electron. Syst. Mag.*, 2017, **32**, pp. 4–16
[6] Saavedra, Z., Argota, J.N., Cabrera, M.A., *et al.*: 'A new approach to OTH main parameters determination', *Radioengineering*, 2019, **28**, (3), pp. 643–650
[7] Pederick, L. H., Cervera, M. A.: 'Modeling the interference environment in the HF band', *Radio Sci.*, 2016, **51**, pp. 82–90
[8] Richards, M.A.: '*Fundamentals of radar signal processing*' (McGraw-Hill, New York, 2014, 2nd edn.)
[9] De Maio, A., De Nicola, S., Huang, Y., *et al.*: 'Design of phase codes for radar performance optimization with a similarity constraint', *IEEE Trans. Signal Process.*, 2009, **57**, (2), pp. 610–621
[10] Sulzer, M.P., Woodman, R.F.: 'Quasi-complementary codes: a new technique for MST radar sounding', *Radio Sci.*, 1984, **19**, (1), pp. 337–344
[11] Golay, M.: 'Complementary series', *RE Trans. Inf. Theory*, 1961, **7**, (2), pp. 82–87
[12] Frank, R.L.: 'Polyphase codes with good nonperiodic correlation properties', *IEEE Trans. Inf. Theory*, 1963, **9**, (1), pp. 43–45
[13] Anderson, S.J.: 'Target classification, recognition and identification with HF radar'. Proc. of the NATO Research and Technology Agency Sensors and Electronics Technology Panel Symp., Oslo, Norway, October 2004
[14] Nitzberg, R.: 'Clutter map CFAR analysis', *IEEE Trans. Aerosp. Electron. Syst.*, 1986, **AES-22**, (4), pp. 419–421
[15] Khan, R.H.: 'Ocean-clutter model for high-frequency radar', *IEEE J. Ocean. Eng.*, 1991, **16**, (2), pp. 181–188